Determinants of DNA Bending in the DNA−Cyclic AMP Receptor Protein Complexes in *Escherichia coli*†

Shwu-Hwa Lin and J. Ching Lee*

Department of Human Biological Chemistry and Genetics, The University of Texas Medical Branch at Galveston, Galveston, Texas 77555-1055

Received December 2, 2002; Revised Manuscript Received February 10, 2003

ABSTRACT: The activated *Escherichia coli* cAMP receptor protein, CRP, is capable of regulating the expression of more than 20 genes by binding to specific DNA sites. DNA bending is an important structural feature that has been observed in the regulatory mechanism of gene expression by CRP. On the basis of the results of the fluorescence energy transfer study of the *gal* P1 promoter, *gal* bends asymmetrically upon binding to CRP, although DNA bends symmetrically in the CRP−*lac* complex. The flanking sequence proximal to the TGTGA motif is involved in a sharper bend than the other side with an overall bending angle of ∼90−125°, without wrapping around the CRP molecule. To understand the factors that control the symmetry in DNA bending, a series of DNA sequences was tested to dissect the contribution of half-sites and flanking sequences, using the natural *gal* P1 and *lac* P1 sequences as initial targets. The extent of DNA bending induced by CRP was monitored by the difference in fluorescence anisotropy between free DNA and the DNA−CRP complex. The extent of bending was sequence-dependent, and most importantly, the symmetry of bending was a function of the symmetry of the DNA sequence. For example, in the *lac* promoter the two binding half-sites (TGTGA and TCACT) were almost symmetric as an inverted repeat. The recognition F-helices of the two CRP subunits would bind to these half-sites with a 2-fold symmetry. The flanking sequences (ATAAA and CATTA) were almost identical mirror images. Thus, they are expected to bend in a similar manner. Finally, the sequence symmetry properties of a series of natural CRP promoters were analyzed. A strong tendency for symmetry sequence was encoded in class I promoter sites but not in class II promoter sites. Results from this analysis support the conclusion that the geometry of the CRP−DNA complex plays a major role in determining the molecular mechanism in gene transcription.

CRP[1] selectively controls more than 20 genes in *Escherichia coli*. Induced DNA bending is an integral part of the mechanism of CRP activation of gene transcription. The CRP-induced DNA bending was originally recognized from nondenaturing gel electrophoretic analysis of the protein−DNA complex (*1*−*3*), and was then mapped to a locus near the center of the binding site by Wu and Crothers (*3*). It was predicted that CRP induces DNA bending with a sharp bend of 100−160°, based on a DNA−CRP model constructed by fitting the B-DNA structure to the protein electrostatic potential (*4*). This prediction is in good agreement with the deduced bend of 100−140°, based on results from studies of electrophoretic mobility in polyacrylamide gels (*5*, *6*). To determine the precise interactions of CRP with its DNA binding site and to explore the nature and extent of CRP-induced distortion of DNA, Steitz and coworkers (*7*) surveyed a wide range of conditions and DNA sequences for crystallizing a CRP−DNA complex. They published the 3 Å resolution crystal structure of CRP complexed with a DNA 30 bp in length. Sequences of the two half-sites that correspond to the DNA sequence of −26 to −41 in the *gal* promoter were employed to produce an effective length of 30 bp with 5′-dG base overhangs. The overall DNA bending induced by CRP is ∼90°, with symmetrical 40° kinks between base pairs 5 and 6 on each side of the dyad axis.

The promoters regulated by CRP can be categorized into three classes, depending on the location of the CRP binding site in relationship with its distance from the transcription start site. In class I, typified by the *lac* promoter, the CRP binding site is located at base pair −61, upstream of the start site, whereas in class II, typified by the *gal* promoter, the CRP binding site is located at base pair −41. The location of the CRP binding site should have major implications on its interaction with RNA polymerase.

Current understanding indicates that the proper orientation of CRP for possible interaction with RNA polymerase may result in upstream DNA contacts with RNA polymerase to activate the transcription (*8*−*10*). RNA polymerase is capable of distinguishing between class I and class II promoter sites by making a different set of contacts between CRP and RNA polymerase in the presence of the promoter site (*11*−*13*),

† Supported by NIH Grant GM 45579 and by Robert A. Welch Foundation Grants H-0013 and H-1238.

* To whom correspondence should be addressed. Telephone: (409) 772-2281. Fax: (409) 772-4298. E-mail: jclee@utmb.edu.

[1] Abbreviations: CRP, cyclic AMP receptor protein; FM, fluorescein 5-maleimide; CPM, 7-(diethylamino)-3-(4-maleimidylphenyl)-4-methylcoumarin; TEK(100) buffer, 40 mM Tris, 100 mM KCl, and 1 mM EDTA at pH 7.8 and 25 °C; FRET, fluorescence resonance energy transfer.

10.1021/bi027259+ CCC: $25.00
Published on Web 04/05/2003

which may be a consequence of different degrees of DNA bending induced by CRP. There is, however, no direct supporting evidence, although DNA sequences modulating the extent of protein-induced bending were elucidated by the study by Garterberg and Crothers (*14*). Several lines of evidence in the literature have indicated that DNA bends symmetrically in the CRP−DNA complex (*1*, *3*, *7*, *15*, *16*), despite asymmetric structural feature in the CRP system (*17*−*20*). CRP-induced symmetric and asymmetric bending of *lac* and *gal* sequences, respectively, have recently been reported in fluorescence studies (*15*, *21*). On the basis of this observation, the authors proposed that the bending geometry might be related to the difference in the molecular mechanism of interaction between CRP and DNA in class I and class II CRP binding sites. This study addresses the issue of the bending geometry in the *gal* promoter and identifies the determinants which define the bending geometry.

MATERIALS AND METHODS

Chemical

Deprotected and desalted oligodeoxyribonucleotides were purchased from Genosys (Genosys Biotechnologies, Inc., The Woodlands, TX). The fluorescent probes CPM and FM were purchased from Molecular Probes. Other reagents and buffer materials were purchased from either Sigma or Boehringer Mannheim.

CRP Preparation

CRP was isolated and purified from an overproducing strain of *E. coli* by the method described in Heyduk and Lee (*20*). Protein was stored in a buffer containing 50 mM PO_4^{3-}, 100 mM KCl, 1 mM EDTA, 1 mM DTT, and 10% glycerol at pH 7.5 and −20 °C. CRP was routinely dialyzed against the desired buffer and was gently filtered through a membrane with a pore size of 0.22 μm before being used.

DNA Preparation

Single-strand oligonucleotides were purified by denaturing PAGE (12−15% acrylamide and 7.5 M urea) and labeled specifically at the 5′-end with CPM or FM by the method described by Heyduk and Lee (*15*, *20*). The free probe was removed by extensive dialysis against TE buffer [50 mM Tris and 1 mM EDTA (pH 7.8)]. The degree of labeling was calculated from the absorption spectrum of the single-strand oligonucleotides, ranging from 0.65 to 0.95 mol of CPM/mol of DNA and from 0.85 to 0.97 mol of FM/mol of DNA. The CPM-labeled single-strand oligonucleotides were annealed with the appropriate complementary strands. The integrity of the CPM-labeled double-strand oligonucleotides (CPM-dsDNA) was monitored by fluorescence anisotropy, since CPM-ssDNA and CPM-dsDNA have different anisotropies. The DNA annealing procedure was repeated as necessary with the addition of appropriate complementary strand oligonucleotides until the anisotropy of the DNA sample reached the maximum for CPM-dsDNA. At this point, no CPM-ssDNA existed in the sample. Finally, the samples were dialyzed against TE buffer and stored at −20 °C.

Doubly labeled DNA (FM-DNA-CPM) was prepared by annealing CPM-labeled single-strand oligonucleotides with an excess amount of FM-labeled single-strand oligonucleotides. The integrity of the CPM-DNA-FM labeled double-strand oligonucleotides was also monitored by anisotropy as described above.

Solution concentrations were determined from the absorption spectrum with the following extinction coefficients: 20 400 M^{-1} cm^{-1} at 278 nm for the CRP monomer (*22*), 14 650 M^{-1} cm^{-1} at 258 nm for cAMP (*23*), 33 000 M^{-1} cm^{-1} at 387 nm for CPM (*21*), and 80 000 and 27 000 M^{-1} cm^{-1} at 494 and 260 nm, respectively, for fluorescein attached to dsDNA at pH 7.8 (based on a value of 83 000 M^{-1} cm^{-1} at 492 nm and pH 9.0 for fluorescein; Molecular Probes). Absorption spectra were measured with a Hitachi U-2000 spectrophotometer.

Fluorescence Anisotropy Titration

The affinity between CPM-dsDNA and CRP was obtained from the anisotropy titration of CPM-labeled dsDNA (10−15 nM) with CRP in TEK(100) buffer containing 200 μM cAMP. The SLM 8000C spectrofluorometer was set as described by Pyles et al. (*24*). The reaction scheme best describing the global binding of CRP to DNA was discussed previously (*19*, *25*, *26*). The observed variation of fluorescence anisotropy with protein concentration was analyzed on the basis of the following equation:

$$A_{obs} = A_D + \Delta A x\,[K_{app}D_T + K_{app}P_T + 1 - \sqrt{(K_{app}D_T + K_{app}P_T + 1)^2 - 4K_{app}{}^2D_TP_T}]/[2K_{app}D_T] \quad (1)$$

where K_{app}, A_{obs}, A_D, ΔA, P_T, and D_T are the apparent association constant, the observed anisotropy, the anisotropy of free DNA, the total change in anisotropy, and the total protein and DNA concentrations, respectively. At least two titrations were performed for each CRP−DNA interaction that was examined, and the curves were nonlinearly fit to the observed data with eq 1 by using Sigmaplot (Jandel Scientific Software, San Rafael, CA).

FRET (Fluorescence Resonance Energy Transfer) Analysis

Measurement. All fluorescence measurements were performed in TEK(100) containing 200 μM cAMP at pH 7.8 and 25 °C. Steady-state fluorescence was recorded on a SLM 8000C spectrofluorometer. Fluorescence spectra were collected with the excitation and emission polarizer set at "magic angles" to eliminate polarization effects (*27*).

Sensitized fluorescence measurement (energy transfer from Trp to CPM) was conducted as described by Heyduk and Lee (*15*) with slight modifications. The concentration of DNA in this type of study was ∼50 nM, while the CRP concentration was between 1.2 and 3.5 μM to make sure that the DNA−CRP complex was well-formed. Spectra were corrected for buffer scattering and sample dilution with the addition of CRP. Two corrected excitation spectra were individually recorded from 260 to 310 nm and from 350 to 450 nm with different PMT voltage settings, while the emission was being monitored at 500 nm. Thus, a low count rate in the UV range could be avoided, and a high signal-to-noise ratio could be reached. The measurement for

apparent efficiency of energy transfer, defined as the ratio of fluorescence intensity integrated in the range of 284−290 nm with and without CRP, was used. A value of >1 indicates the presence of energy transfer. This value was corrected for a change in CPM fluorescence induced by CRP binding when CPM was excited above 320 nm, where protein absorption is negligible. The ratio of fluorescence intensity integrated in the range of 385−410 nm with and without CRP was employed to assess the effect of CRP binding. This correction did not exceed 5% of the signal.

The measurement of the fluorescence intensity decay of the CPM attached to DNA was carried out on a LTD single-photon counting spectrometer (IBH Consultants, model 5000U) in H. C. Cheung's laboratory at the University of Alabama at Birmingham (Birmingham, AL). The excitation light was set at 390 nm, and the emitted light selected by a monochromator was set at 475 nm. The photons were accumulated for 10 000 or 20 000 counts for each set of samples. Ludox was used to collect the lamp profile. The concentration of DNA in this type of study was ~500 nM, and the concentration of CRP was between 2 and 3.5 μM to ensure that the DNA−CRP complex was well-formed. All stock DNA samples for fluorescence lifetime decay measurement were dialyzed with TEK(100) buffer prior to lifetime measurements to avoid alteration of the salt concentration. The intensity decay of the donor (CPM) is not monoexponential, so analysis of the donor-only and donor−acceptor decay was carried out with the multiexponential model

$$I(t) = \sum_i \alpha_i \exp\left(-\frac{t}{\tau_i}\right) \tag{2}$$

where α_i values are the fractional amplitudes associated with the decay times τ_i. The average donor lifetime, $\langle\tau\rangle$, was calculated with the equation

$$\langle\tau\rangle = \frac{\sum_{i=1}^{n} \alpha_i \tau_i}{\sum_{i=1}^{n} \alpha_i} \tag{3}$$

Energy Transfer Analysis. The efficiency of energy transfer (E) between CPM and FM was calculated by measuring the steady-state fluorescence (F) and fluorescence lifetimes of a donor in the absence (d) and in the presence of acceptor (da) according to the following equation

$$E = \frac{R_0^{\,6}}{R_0^{\,6} + R^6} = 1 - \frac{F_{da} - F_d(1 - f_a)}{F_d f_a} = 1 - \frac{\tau_{da}}{\tau_d} \tag{4}$$

Since the labeling of donor and acceptor was not stoichiometric, f_a, the observed degree of labeling of the acceptor site, was used as a correction factor when calculating the transfer efficiency (*28*). In the study presented here, the labeling degree of the acceptor (FM) exceeded that of the donor (CPM), implying that every donor molecule participates in the energy transfer. Therefore, the transfer efficiency obtained from lifetime measurement is not affected by nonstoichiometric labeling. The Förster distance, R_0, was calculated by using the spectral properties of the donor and acceptor fluorophores:

$$R_0^{\,6} = (8.79 \times 10^{-5})(n^{-4} Q_d \kappa^2 J) \tag{5}$$

The range of the orientation factor (κ^2) was estimated by limiting anisotropy, which was determined from the Perrin plots (*29*). The viscosity of the solution was varied with addition of glycerol (*30*). The value for the limiting anisotropy was 0.335 when the donor (CPM) was attached to *gal*-50 in either the CRP−*gal*-50/-25 or CRP−*gal*-50/-29 complex. Values of 0.153 and 0.208 were observed for the acceptor (FM) attached to *gal*-25 and *gal*-29 in the CRP−*gal*-50/-25 and CRP−*gal*-50/-29 complexes, respectively. The refractive index (n) of the solution was taken to be 1.4. The fluorescence quantum yield of CPM (Q_d) was previously measured to be 0.86 by Heyduk and Lee (*15*). J (M^{-1} cm^{-1} nm^4), the spectrum overlap integral between the corrected emission spectrum of the donor-labeled sample, $F_D(\lambda)$, and the absorption spectrum of the acceptor in donor/acceptor samples, $\epsilon_A(\lambda)$, was approximated by

$$J = \frac{\sum F_D(\lambda)\epsilon_A(\lambda)\lambda^4 \Delta\lambda}{\sum F_D(\lambda)\Delta\lambda} \tag{6}$$

To obtain the corrected emission spectrum, the correction factor of the instrument was obtained by comparing the emission spectrum of 200 μM β-naphthol in 20 mM acetate buffer at pH 4.75 and 25 °C with the corrected spectrum of β-naphthol (*31*). The overlap integral was calculated by numerical integration, and a J of 4.05×10^{14} was obtained with a 1 nm interval.

RESULTS

To use fluorescence resonance energy transfer (FRET) to estimate the extent of CRP-induced *gal* bending, the best location for the attachment of the donor and acceptor was determined. Design of the DNA segment and the donor location were determined on the basis of the following criteria. First, the donor is placed at the same location in a series of *gal* segments to eliminate the possibility that the fluorescence signal senses the environmental change and does not primarily reflect the results of FRET. Second, without a reduction in the affinity between DNA and CRP, the donor is covalently attached to the DNA as close as possible to the kink point to decrease the error in estimating the bending angle, because CRP-induced DNA bending results from two kinks at the two half-binding sites (*7*). The end of the flanking sequence distal to the TGTGA motif was chosen as a location to which to attach the donor, since in the CRP−*gal* complex the flanking sequence proximal to the TGTGA motif is involved in greater bending than the flanking sequence distal to the TGTGA motif (*21*). Finally, a suitable length of DNA is determined so that the end-to-end distance can be measured by using FM and CPM as the donor and acceptor, respectively (R_0 = 41.8 Å base on $\kappa^2 = {}^2/_3$). A series of *gal* segments in which the specific CRP binding site is not located in the center was designed so that the flanking sequence proximal to the TGTGA motif is longer than the other side. These sequences were coded with two

Table 1: Binding Parameters for Formation of the Complex of CPM-Labeled *gal* Segments and CRP[a]

sample	length (bp)	CPM location	ΔA	K_{app} ($\times 10^6$ M^{-1})	CPM location	ΔA	K_{app} ($\times 10^6$ M^{-1})
gal-29/-54	26	−29	0.064	13.45 ± 3.18	−54	0.040	8.25 ± 0.64
gal-27/-52	26	−27	0.039	10.00 ± 0.28	−52	0.040	11.40 ± 1.41
gal-25/-50	26	−25	0.040	4.35 ± 0.35	−50	0.056	10.80 ± 2.40
gal-23/-48	26	−23	0.040	1.30 ± 0.01	−48	0.063	3.10 ± 0.28
gal-29/-50	22	N/A	N/A	N/A	−50	0.054	2.38 ± 0.01
gal-25/-50	26	−25	0.040	4.35 ± 0.35	−50	0.056	10.80 ± 2.40
gal-19/-50	32	−19	0.029	4.20 ± 0.28	−50	0.055	14.24 ± 2.05
gal-11/-50	40	−11	0.027	1.45 ± 0.07	−50	0.054	13.35 ± 1.34

[a] The experimental conditions for these experiments are given in Figure 2. The values of the apparent binding constant (K_{app}) and the total anisotropy change (Δ*A*) were recovered from fitting the data to eq 1. The values are given as means ± the standard deviation of the best-fitted values obtained from two to four different titrations. The standard error was in the range of 0.001−0.002 for Δ*A* for all samples in the curve fitting.

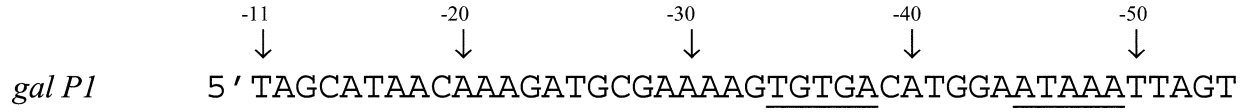

FIGURE 1: Sequence of the *gal* P1 fragment employed in this study. The sequence is from the 5′-end to the 3′-end. CRP binding sites are underlined. The numbers above the sequence indicate the distance in base pairs relative to the transcriptional start site.

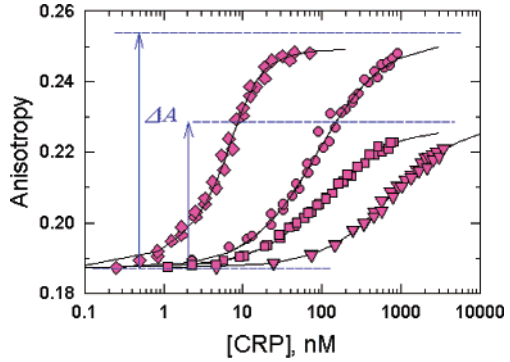

FIGURE 2: Typical anisotropy titration of CPM-labeled DNA with CRP. The change in anisotropy is plotted against the logarithm of total CRP concentration. The data were fitted to eq 1, where K_{app} is the apparent binding constant and Δ*A* is the total anisotropy change between free DNA and the DNA−CRP complex. The recovered parameters are summarized in Tables 1 and 5.

numbers that denote the initial and last base pairs relative to the transcriptional start site; e.g., *gal*-29/-54 is a 26 bp DNA that has a sequence corresponding to base pairs −29 to −54 of the *gal* promoter. The sequence of *gal* is shown in Figure 1.

Affinity Control

Fluorescent anisotropy titration of CPM-labeled DNA with CRP was previously used to monitor the interaction between CRP and DNA in different operons (*25*). The same method was adopted in this study to estimate the apparent affinity between the *gal* segments and CRP. Typical titration curves are shown in Figure 2, and the results are listed in Table 1. All the observed fluorescence anisotropy values are lower than the limiting anisotropy of CPM in the CRP−*gal*-50/-25 complex (Materials and Methods), implying that the anisotropy observed here is not affected by any artifacts, such as scattering caused by aggregation. When CPM is attached to *gal*-54, *gal*-52, and *gal*-50 in the 26 bp oligomers, the affinities are similar. The apparent affinity decreases 70% when CPM is attached to *gal*-48 in the *gal*-23/-48 segment. This result indicates that attachment of a probe to *gal*-48 interferes with protein−DNA interaction. *gal*-50 was chosen as the location for the donor in the end-to-end FRET study, not only because it maintains the affinity level but also because it is close to the kink point. The affinities between CRP and *gal* segments with different lengths with *gal*-50 at one of the end positions were also studied, and the results are listed in Table 1. *gal*-50/-25 (26 bp), *gal*-50/-19 (32 bp), and *gal*-50/-11 (40 bp) have the same affinity with CRP (>10 $\times$ 10^6 M^{-1}). However, if the length of the DNA segment decreases to 22 bp (*gal*-50/-29), the affinity decreases to 2.4 $\times$ 10^6 M^{-1}.

The effect of placing the CPM at the opposite end was tested by monitoring the affinities of CRP for these *gal* segments. The results are also listed in Table 1. With 26 bp oligomers, g*al*-29/-54 and *gal*-27/-52 have similar apparent affinities, but the affinity decreases to ∼50% with *gal*-25/-50 and ∼10% with *gal*-23/-48. With segments of different lengths, *gal*-50/-25 (26 bp) and *gal*-50/-19 (32 bp), similar but lower affinities were observed. However, the affinity decreases significantly with an increase in the length of the DNA segment up to 40 bp.

Results of these measurements establish the limits on the lengths of particular segments and the placement of the probe that can be employed in this study.

End-to-End FRET Study

End-to-End FRET. Four different lengths of DNA sequence that contain the *gal* promoter (*gal*-29/-50, *gal*-25/-50, *gal*-19/-50, and *gal*-11/-50) were employed in the end-to-end FRET study. The donor, CPM, was placed at *gal*-50, and the acceptor, FM, was labeled at the other end. The efficiency of energy transfer was estimated with steady-state fluorescence and fluorescence lifetime decay of the donor. Fluorescence decay of the CPM-labeled DNA−CRP complex was best fit with a two-exponential function (eq 2), resulting in two lifetimes with and without the acceptor (Table 2). Data shown here were obtained from a single measurement. However, multiple runs were performed for each sample, and the averaged data are shown as means in the sixth column of Table 2. The donor-only samples reveal the same lifetime (mean value) within the experimental error range. The efficiency of fluorescence energy transfer was calculated

Table 2: Intensity Decay of CPM in the DNA−CRP Complex[a]

sample	τ_i (ns)	α	$\langle\tau\rangle$ (ns)	χ_R^2	mean ± SD
gal-29/-50 (d)	0.92	0.28			
	3.71	1.29	3.21	0.94	3.26 ± 0.06
gal-29/-50 (d + a)	0.83	0.52			
	3.49	1.36	2.75	0.81	2.78 ± 0.05
gal-25/-50 (d)	0.94	0.20			
	3.70	1.18	3.30	0.97	3.32 ± 0.04
gal-25/-50 (d + a)	0.83	0.33			
	3.60	1.23	3.01	1.24	3.05 ± 0.07
gal-19/-50 (d)	1.06	0.23			
	3.69	1.09	3.22	0.87	3.26 ± 0.08
gal-19/-50 (d + a)	0.90	0.26			
	3.68	1.11	3.15	0.77	3.21 ± 0.06
gal-11/-50 (d)	0.87	0.36			
	3.69	1.33	3.09	0.93	3.11 ± 0.08
gal-11/-50 (d + a)	0.90	0.30			
	3.62	1.13	3.05	0.87	3.10 ± 0.07

[a] (d) denotes DNA labeled with donor alone, and (d + a) denotes DNA labeled with both the donor and acceptor. These decay data were fitted with a biexponential function, with lifetimes (τ_i), and the associated fractional amplitudes (α_i). $\langle\tau\rangle$ is the average lifetime and calculated from eq 2. The DNA concentration is ∼500 nM, and the protein concentration is ∼2−3 μM. Measurements were taken in TEK(100) buffer with 200 μM cAMP at pH 7.8 and 25 °C. Each measurement was performed two or three times. The averaged data and the standard deviation from different measurements are shown in the sixth column. The mean values were used to calculate the efficiency of FRET, and the result is listed in Table 3.

Table 3: Summary of the End-to-End FRET Study[a]

sample	length (bp)	efficiency of FRET (E) steady-state	efficiency of FRET (E) lifetime	$\langle\kappa^2\rangle$	R_0 (Å)	R (Å)
CRP−*gal*-29/-50	22	22.1%	14.7 ± 3.6%	3.08 (max)	53.9	76.5
				$^2/_3$	41.8	56.2
				0.121 (min)	31.4	42.2
CRP−*gal*-25/-50	26	13.5%	8.1 ± 3.5%	2.82 (max)	53.1	79.6
				$^2/_3$	41.8	62.7
				0.156 (min)	32.8	49.2
CRP−*gal*-19/-50	32	6.2%	1.5 ± 4.3%			
CRP−*gal*-11/-50	40	1.0%	0.3 ± 4.8%			

[a] The end-to-end FRET was investigated by the steady-state fluorescence and the lifetime decay of donor. The efficiency of FRET was estimated according to eq 4. The range of the orientation factor $\langle\kappa^2\rangle$ was calculated from the depolarization factor of the donor and acceptor through the measurements of limiting anisotropy of probes. The distances between CPM and FM in the CRP−*gal*-29/-50 and CRP−*gal*-25/-50 complexes are estimated from the efficiency of FRET based on fluorescence lifetime decay data. However, the donor−acceptor distances in 32 and 40 bp oligomer were not estimated since the efficiency of energy transfer was low.

with the average lifetime as listed in Table 3. The efficiency of FRET decreases with an increase in the length of the DNA segment. A similar pattern was observed with steady-state fluorescence study. Comparing the lifetime of donor decay in the CRP−*gal*-29/-50 complex with and without the acceptor yields a 14.5% energy transfer, which corresponds to a donor−acceptor distance of 56 Å (R_0 = 41.8 Å base on $\kappa^2 = {}^2/_3$). When the length of DNA is 26 bp (*gal*-25/-50), the efficiency of energy transfer is 8.1%, corresponding to a donor−acceptor distance of 63 Å.

Calculation of R_0. An R_0 of 50 Å has previously been evaluated for CPM and FM (*15*). When CPM was attached to *lac*-74 or *lac*-54, the emission spectrum of CPM was not affected by the addition of CRP, but a 4.5 nm blue shift was observed with the CRP−*gal* segment that has the probe CPM attached at *gal*-50. It is possible that CPM at this location is close to the protein molecule, and therefore, it easily senses a change in the environment when DNA fragments interact with CRP. The blue shift in the emission spectrum causes the decrease in the overlap integral (J) between CPM and FM, thus decreasing the value of R_0. On the basis of the value of limiting anisotropy, the probe attached to *gal*-50 has less local mobility than the probe attached to *lac* (*15*). Therefore, the range of the orientation factor was estimated (*28*). Substituting a J of 4.05×10^{14} M^{-1} cm^{-1} nm^4, an n of 1.4, a Q_d of 0.86, and the orientation factor into eq 4, we can derive R_0 values (listed in Table 3). These values closely correlate with R_0 values observed for coumarin (CPM)-fluorescein, which lie between 27 and 52 Å with various values for the orientation factor (*32*).

Table 4: Summary of the Sensitized Fluorescence Study[a]

sample	CPM location	n	apparent efficiency of FRET	CPM location	n	apparent efficiency of FRET
gal-29/-54	−29	3	1.21 ± 0.01	−54	4	1.12 ± 0.02
gal-27/-52	−27	4	1.09 ± 0.02	−52	2	1.06 ± 0.02
gal-25/-50	−25	3	1.02 ± 0.01	−50	4	1.13 ± 0.01
gal-23/-48	−23	3	1.01 ± 0.01	−48	2	1.02 ± 0.01
gal-19/-50	−19	3	1.02 ± 0.01	−50	4	1.12 ± 0.02
gal-11/-50	−11	4	0.99 ± 0.02	−50	3	1.12 ± 0.01

[a] Fluorescence energy transfer from Trp in CRP to CPM attached to DNA was monitored by sensitized fluorescence. The details of the experimental conditions and data calculation are described in Materials and Methods. An apparent efficiency of FRET was obtained as the ratio of fluorescence intensity with and without CRP added. This value was corrected for a change in CPM fluorescence induced by CRP binding.

FRET Study from Tryptophan to CPM

FRET between the DNA End and Protein. Sensitized fluorescence studies were conducted to further define the DNA bending geometry, and the results are listed in Table 4. CRP contains two tryptophan residues (Trp13 and Trp85) per subunit, and they are located at α-helix A and β-strand 7, respectively (*33*). Since the emission spectrum of Trp overlaps with the absorption spectrum of CPM, it is possible to use Trp and CPM as the donor and acceptor, respectively, to perform the FRET study to monitor the distance between the end of the DNA segment and the Trp residues in CRP. When CPM is attached to the end of the flanking sequence proximal to the TGTGA motif, the apparent efficiency of energy transfer from Trp to CPM decreases while the location of the acceptor is changed from *gal*-29 to *gal*-27 to *gal*-25. There is almost no detectable energy transfer from Trp to CPM, when CPM is located at *gal*-25, *gal*-23, *gal*-19, and *gal*-11. When CPM was attached to the other end of the DNA segment, the efficiency of transfer between Trp and CPM in four locations (*gal*-48, *gal*-50, *gal*-52, and *gal*-54) were tested. Essentially the same apparent efficiency result was observed, although the efficiency was marginally lower for *gal*-48 and *gal*-52, the significance of which is not known at present.

Symmetry of CRP-Induced DNA Bending

Symmetry of CRP-induced DNA bending was previously studied by comparing the enhancement of sensitized fluorescence with CPM attached to different ends of DNA (*15*,

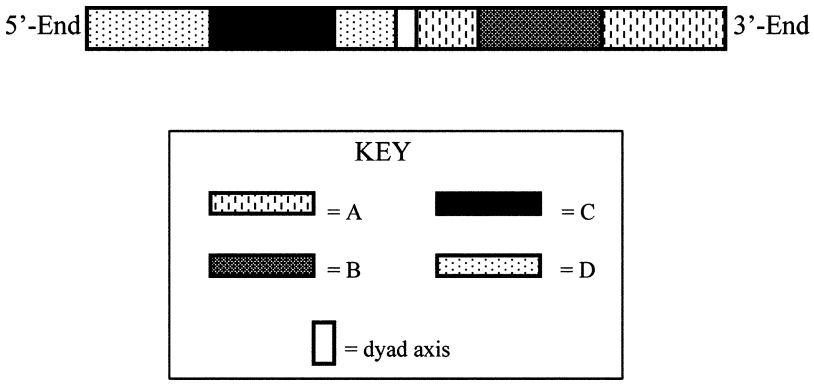

FIGURE 3: Cartoon of CRP binding sites. Specific regions within the CRP binding site are highlighted and annotated in the figure: (A) flanking sequence distal to the conserved TGTGA motif, (B) inverted repeat motif, (C) conserved TGTGA motif, and (D) flanking sequence proximal to the conserved TGTGA motif.

Table 5: Extent of DNA Bending and Association Constants for the CRP−DNA Complex

DNA sequence[e]	proximal[a]			distal[b]		
	ΔA[c]	FRET[d]	K_{app} ($\times 10^6$ M^{-1})[c]	ΔA[c]	FRET[d]	K_{app} ($\times 10^6$ M^{-1})[c]
LCLL	0.042		74	0.041		53
LCGL	0.060		1.13	0.063		1.27
LCLL	0.042		74	0.041		53
LCLR	0.047	1.16 ± 0.03	48.3	0.038	1.13 ± 0.02	48.2
RCLR	0.052		4.3	0.050		4.8
GCLG	0.065		606	0.041		314
GCGG	0.065	1.21 ± 0.01	15.7	0.040	1.12 ± 0.02	8.7
GCGR	0.065		10.8	0.038		8.1
RCGG	0.056		2.05	N/A		N/A
LCGL	0.060		1.13	0.063		1.27

[a] CPM was attached to the flanking sequence proximal to the TGTGA motif. [b] CPM was attached to the flanking sequence distal to the TGTGA motif. [c] Apparent association constants of CRP binding to DNA and the total anisotropy change for the formation of the CRP−DNA complex were obtained from fluorescence anisotropy titration experiments as described in the legend of Figure 2. [d] The apparent efficiency of FRET between Trp in CRP and CPM attached to DNA was estimated from the desensitized fluorescence study. [e] A four-letter code is adopted to represent the sequence of CRP binding sites as described in the text. The random sequences are CTCAG and CCCAG for the flanking sequence proximal to and distal to the TGTGA motif, respectively.

21). In the study presented here, the total anisotropy change (ΔA) for formation of the CRP−DNA complex was adopted to estimate the extent of bending of DNA and consequently to determine the symmetry of DNA bending. The fluorescence anisotropy titration of CPM-labeled DNA with CRP was performed to obtain ΔA as reported in Figure 2. The advantage of anisotropy titration is that the affinity of CRP with DNA and ΔA can be obtained at the same time from one experiment. DNA bending by CRP was tested on a series of 26 bp oligonucleotides with natural *lac* and *gal* promoters as a target. Sequences containing the CRP binding sites were synthesized with the recognition sites centrally located in the strand, as shown in Figure 3. Each of the flanking sequences and the recognition motifs have the same number of nucleotides. A four-letter code was adopted to represent the sequences, as reported by Pyles et al. (*24*). In summary, C, L, G, and R represent the conserved TGTGA motif, *lac*, *gal*, and random sequence, respectively. Therefore, LCLL and GCGG represent CRP binding sites in natural *lac* and *gal* promoters. The fluorescent probe, CPM, was covalently attached to the 5′-end of the DNA segment located either at the proximal or distal end of the TGTGA motif. Two parameters, ΔA (total anisotropy change in the formation of the CRP−DNA complex) and K_{app} (the apparent association constant between DNA and CRP), were recovered from the curve fitting of the anisotropy titration data, and the results are listed in Table 5. K_{app} is strongly dependent on the sequence of DNA but is not affected by the location of CPM, since similar affinity is obtained with CPM attached to either end of DNA. However, ΔA is strongly dependent on the DNA sequence and location of the probe. Comparing LCLL with LCGL and RCLR reveals an inverse correlation between ΔA and K_{app}; i.e., a higher ΔA correlates with a lower K_{app}.

DISCUSSION

Geometry of the CRP−gal Complex

Bending Angle Estimated by FRET. In the crystal structure of a CRP−DNA complex, kinks were observed, and they are located at positions corresponding to those between *gal*-36 and *gal*-37 and between *gal*-46 and *gal*-47. The geometric relationship of the various DNA segments in the *gal*−CRP complex is depicted in Figure 4. There are 4 bp between *gal*-50 and *gal*-47, the position of the first kink, corresponding to 13.6 Å. The distance between binding half-sites is 10 bp (34 Å). Thus, the flanking sequence proximal to the TGTGA domain is represented by 12 bp in the CRP−*gal*-25/-50 complex, the total length of which is 26 bp. However, the fluorescent probes are attached to the 5′-end of the DNA; hence, at least 5 Å needs be added at each end to account for the distance added by the flexible linker with which the probes are attached to the DNA. The result of the FRET study (Table 3) shows that the end-to-end distance of DNA is 63 Å in the CRP−*gal*-25/-50 complex. The extent of

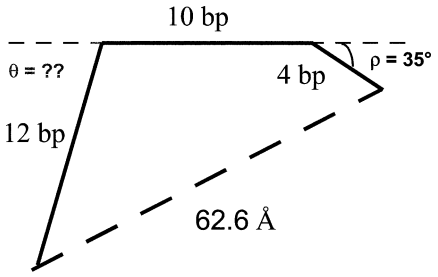

FIGURE 4: Geometry of the CRP−*gal* complex. Solid lines represent *gal*-25/-50. The FRET distance between the donor and acceptor is represented as a dashed line.

bending of the flanking sequence distal to the TGTGA motif has been reported previously by this laboratory to be equivalent of that in the *lac* promoter sequence (*21*). A similar observation is reported in this study since the anisotropy titration experiments yielded the same ΔA value (0.040) for *gal* (Table 5, GCGG) and *lac* (Table 5, LCLL) with CPM attached to the end of the flanking sequence distal to the TGTGA motif. Thus, the extent of bending of this flanking sequence should be the same in *gal* and *lac*. The angle of CRP-induced *lac* bending was previously estimated to be ~35° from a FRET study (*15*). It is compatible with the bending extent of 43° in the crystal structure of the CRP−DNA complex (*7*). Thus, the FRET results provide an end-to-end distance of 63 Å and an angle of bending for the flanking sequence distal to the TGTGA motif of ~35°. Consequently, the bending angle of the flanking sequence proximal to the TGTGA motif relative to the half-binding site segment was estimated to be ~90°. The donor−acceptor distance in the CRP−*gal*-50/-25 complex might be as long as 79.6 Å, if the error in the orientation factor is taken into account (Table 3). Under this condition, a bending angle of 60° was obtained from the calculation. Having estimated that the bending angle at the distal end is ~35°, we find that the overall-CRP induced *gal* bending ranges from 95° to 125°, which agrees well with the value of 100−140° obtained from the electrophoretic mobility in polyacrylamide gels (*5*, *6*). The same result was obtained using the donor−acceptor distance (56.3 Å) in the CRP−*gal*-29/-50 complex to estimate the bending angle. A value of 86° was estimated for the angle between the flanking sequence proximal to the TGTGA motif and the half-binding site motif.

gal Bends without Wrapping around the CRP Molecule. Although the extent of bending of the flanking sequence proximal to the TGTGA motif is as high as 90°, our data do not support the model in which the *gal* is wrapping around CRP. On the basis of the crystal structure of CRP (*33*), the distance from DNA binding sites to the flexible A α-helix, where one of the Trp residues (W13) resides, is ~70 Å. The flanking sequence proximal to the TGTGA motif in the CRP−*gal*-11/-50 complex is 26 bp, corresponding to 88.4 Å. Therefore, DNA fragments employed in this study should be sufficiently long to report whether it is able to wrap around the protein molecule. The other Trp residue (W85) is in β-sheet 7. On the basis of the crystal structure of the CRP−DNA complex (*7*), the distances between position −29 to W13 and W85 are 48 and 33 Å, respectively.[2] The efficiency of FRET increases as the distance between the donor and acceptor decreases. As shown in Table 4, the data indicate a decrease in the level of FRET when CPM was attached to the DNA at different locations such as at *gal*-29, *gal*-27, *gal*-25, *gal*-23, *gal*-19, and *gal*-11. Is it possible that DNA wraps around half the protein molecule so that the CPM (acceptor) has no chance to be close to the Trp (W13) located at α-helix A? If it is the case, the efficiency of energy transfer in the end-to-end FRET study will decrease to and remain constant at a certain level while the flanking sequence wraps around the CRP molecule. The efficiency in the end-to-end FRET study significantly decreases as the length of DNA increases from 22 to 40 bp (Table 3). It was reported that W13 is substantially solvent exposed and contributes to approximately 80% of the Trp fluorescence, while W85 is buried in the matrix of CRP and contributes to roughly 20% of the Trp fluorescence signal (*34*). The significantly greater contribution of W13 should enhance the probability of detecting FRET, and yet a decrease was observed. Hence, the data shown here suggest that the end of *gal* extends away from the protein with increasing length of the flanking sequence of DNA. One may conclude that the flanking sequence of *gal* bends sharply but does not wrap around the protein molecule in the *gal*−CRP complex.

Sequence, Structure, and Stability

Qualitative Estimates of the Extent of DNA Bending by Anisotropy. Fluorescence anisotropy is highly dependent on the viscosity of the solution, size, and shape of the macromolecule (overall rotational diffusion of the macromolecule), as well as the local mobility of the fluorophore. The effect of viscosity is not a factor in this comparative study because the buffer system was kept constant in all anisotropy titration experiments. Hence, the total anisotropy change, ΔA, for the formation of the CRP−DNA complex reports the change in the size, shape, and local mobility of CPM. The effect of size would contribute to the same extent to ΔA as listed in Table 5, since the DNA sequence was kept at 26 bp in this study. Therefore, a difference in ΔA reflects a different shape change as well as a different extent of local mobility change for CPM in the formation of the CRP−DNA complex. The change in the local mobility of CPM significantly contributes to ΔA. For example, the limiting anisotropy of CPM is 0.315 (data not shown) and 0.335 (Materials and Methods) with the probe attached to the −50 position in *gal*-25/-50 and the CRP−*gal*-25/-50 complex, respectively. Compared with the total anisotropy change of 0.056, as shown in Table 1, ~40% of ΔA was accounted for by the change in the local mobility of the probe. Previously, the enhancement of sensitized fluorescence from Trp in CRP to CPM attached to the end of DNA was used as a probe to detect the symmetry of CRP-induced DNA bending (*15*). A greater value of enhancement of sensitized fluorescence reflects the shorter distance between Trp (donor) and CPM (acceptor), which is caused by a greater extent of bending of the flanking sequence. In Table 5, columns 3 and 6, the data on enhancement of sensitized fluorescence correlate with ΔA; e.g., $\Delta A \approx 0.039$ and FRET ≈ 1.12, $\Delta A \approx 0.047$ and FRET = 1.16, and $\Delta A \approx 0.065$ and FRET = 1.21. With a greater extent of bending of the flanking sequence, the CPM is closer to the protein molecule, resulting in higher values of ΔA. Thus, ΔA is a valid reporter on the extent of DNA bending. The same value of ΔA was observed

[2] Mentioned by one of the reviewers.

Table 6: Statistical Analysis of Sequence Symmetry in CRP Promoter Sites

Promoter sites [a]	Ref	Sequence [b] Flanking	Binding site			Flanking	Symmetric bp [c]	Total bp [d]	
Class I			↓						
Lac		**C**AATTAA	T**GTGA**	GTTAGC	*TCAC**T***	CATTAG**G**	9	12	75.0%
tnaA		GAACGAT	*TGTGA*	TTCGAT	*TCACA*	T**T**TAA**AC**	8	12	66.7%
ilvB		TAC**AAA**A	C**GT**GA	TCAACC	C**CT**CA	A**TTT**TCC	7	12	58.3%
BglR wt	317	TA**A**T**AA**C	T**G**C**GA**	GCATGG	**TC**AT**A**	T**TTT**T**A**T	9	12	75.0%
ColE1 site1	318	**C**CA**TTTT**	T**GTGA**	AAACGA	**TCAAA**	**AAAA**CA**G**	9	12	75.0%
uxuAB	319	A**A**T**T**GT	T**GTG**A	TGTGGT	**TAAC**C	CA**A**T**T**AG	7	12	66.7%
tdc	320	GTTA**AT**T	**TGTG**A	GTGGTC	***G**CACA*	T**AT**CCTG	9	12	75.0%
									70.2%±6.6%
Class II			↓						
Gal	316	C**G**AA**A**AG	T**G**TG**A**	CATGGA	A**T**AA**A**	TT**A**GT**G**G	8	12	66.7%
deoP2site1	313	CCTTA**A**T	T**GTGA**	TGTGTA	*TC**GAA***	GTGTGTT	5	12	41.7%
pBRP4	316	TATGCGG	**TGTG**A	AATACC	G**CACA**	GATGCGT	7	12	58.3%
CCPmelR	313	A**GGT**AA**A**	**TGTGA**	TGTACA	**TCACA**	**T**GGA**TC**C	8	12	66.7%
pmelR (323)	313	T**GA**A**AC**	C**GTG**C	TCCCAC	T**CG**C**A**	**GT**CA**TC**C	6	12	50.0%
CC	19	A**GGT**AA**A**	**TGTGA**	TGTACA	**TCACA**	**T**GGA**TC**C	8	12	66.7%
cya	322	AAGG**A**GG	T**GTTA**	AATTGA	**TCAC**G	TTT**T**AGA	5	12	41.7%
									54.2%±11.5%

[a] Three classes of CRP binding sites on DNA whose overall mechanisms differ from one another at the molecular level have been identified (*12*, *37*). On the basis of the report by deCrombrugghe et al. (*17*), Berg and von Hippel (*38*) have listed 26 recognition sequences for CRP. Among them, we picked class I and class II CRP binding sites for these analyses. [b] The sequence of CRP binding sites was grouped as flanking sequences, binding sites, and spacers for analysis. The arrows indicate the dyad axes. Bold letters indicate that the base pair is an inverted repeat in both sides through the dyad axis. If the base pair is identical as a mirror image, the sequence is underlined. [c] The base pair in either flanking sequence or binding sites with symmetry property was counted. [d] There are 12 bp in each analyzed sequence, including 7 bp in the flanking sequence and 5 bp in the binding sites.

no matter which end of CPM was attached to *lac* (LCLL in Table 5), suggesting that *lac* bends symmetrically upon binding of CRP. In contrast to the data for the *lac* promoter, a Δ*A* of 0.065 was observed with the *gal* promoter (GCGG in Table 5) when CPM was attached to the flanking sequence proximal to the TGTGA motif and a Δ*A* of 0.040 when CPM was attached to the opposite end. This result suggests that *gal* bends asymmetrically upon binding of CRP and the flanking sequence proximal to the TGTGA motif bends more than the other side, confirming the previous conclusions which were derived by using different parameters (*15*, *21*).

Specificity and Bendability. On the basis of the fluorescence studies, the two flanking sequences of the *lac* promoter bend symmetrically (*15*), but the flanking sequence of *gal* proximal to the TGTGA motif is involved in a sharper bend than the flanking sequence distal to the TGTGA motif upon interacting with CRP (*21*). Analysis of the sequence of these two operons around the CRP binding site shows that the two half-binding sites are almost symmetric as inverted repeats and the two flanking sequences are almost identical as mirror images in the *lac* promoter. However, the *gal* promoter does not have this property (Figure 4). How much does the symmetry of the DNA sequence contribute to the structural stability in the CRP−DNA complex? A series of hybrid 26 bp oligonucleotides with natural *lac* and *gal* promoters as a target were used to investigate the relationship between the symmetry of flanking sequences and the CRP-induced DNA bending. The extent of DNA bending induced by CRP was monitored by the difference of fluorescence anisotropy between DNA and the DNA−CRP complex. In Table 5, in keeping the flanking sequence constant and changing the sequence of the half-binding site, we find the Δ*A* obtained from LCGL (0.060 and 0.063) is much higher than that obtained from LCLL (0.042 and 0.041), but the value of Δ*A* is not affected by the location of CPM. This implies that both DNAs bend symmetrically, but the bending angle of DNA in the CRP−LCGL complex is greater than that in the CRP−LCLL complex. It is necessary to note that the two flanking sequences in LCGL and LCLL are almost mirror images of each other. If one of the flanking sequences is changed with random sequence, LCLR will lose the symmetric bending property, as evidenced by the disparity in the values of Δ*A* (0.047 and 0.038), depending on the location of the probe. The two flanking sequences are not mirror images if they are substituted with the *gal* promoter sequence (GCLG). Asymmetric bending was observed as evidenced by Δ*A* values of 0.065 and 0.041, suggesting that the flanking sequence proximal to the TGTGA motif is involved in a sharper bend than that on the other side in the CRP−GCLG complex. GCLG and GCGG (*gal* promoter) have the same flanking sequences but different DNA recognition sites. The observed Δ*A* supports the idea that the extent of bending of GCLG is the same as that of GCGG. Interestingly, when both sides of flanking sequences of LCLL are substituted with random sequences, RCLR also bends symmetrically with Δ*A* values of 0.052 and 0.050. It is because one base pair is symmetric as a mirror image and three base pairs are invert repeats among the five base pairs of random flanking sequence. The random flanking sequences are described in Table 5. Overall, these data suggest that symmetry in the sequence is a major factor which determines the symmetry of CRP-induced DNA bending.

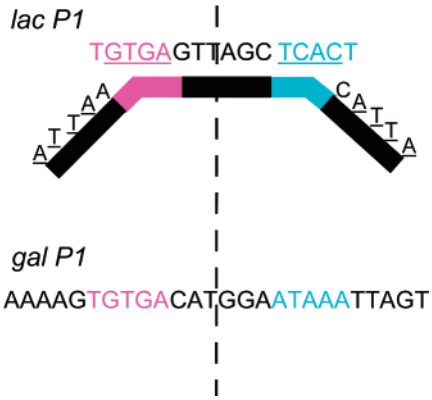

FIGURE 5: Symmetry of the DNA sequence. Two half-binding sites are almost symmetric as inverted repeats, and the two flanking sequences are almost identical as mirror images in the *lac* promoter. However, the *gal* promoter does not have this property.

Correlation between K_{app} and ΔA. As shown in Table 5, when the DNA recognition site LCLL is substituted with *gal*, LCGL bends more than LCLL ($\Delta A = 0.042$ vs 0.060). The affinity decreases by 50-fold, corresponding to values of 64×10^6 and 1.2×10^6 M^{-1} with LCLL and LCGL, respectively. There is an inverse correlation between the extent of bending and binding affinity. This inverse correlation implies that energy is consumed to exert a greater extent of bending in the CRP−LCGL complex. Substituting the DNA recognition site in GCGG with *lac* leads to the sequence of GCLG. GCLG and GCGG have the same extent of bending, with ΔA values of 0.065 and 0.041 when CPM is attached to the flanking sequence proximal to and distal to the TGTGA motif, respectively. The affinities of CRP with GCLG and GCGG are $\sim 460 \times 10^6$ and 12.2×10^6 M^{-1}. Changing the recognition site from GCLG to GCGG leads to a 38-fold decrease in affinity. However, in this case, there is no change in the geometry of binding which remains asymmetric, apparently to the same extent. The combined result implies that energy is probably required in bending to stabilize the conformation of the molecule as reflected by the lower apparent affinity; however, the ability to bend depends on the sequence.

In DNA with a bending propensity like those of GCLG, GCGG, and GCGR, the flanking sequence proximal to the TGTGA motif bends strongly as indicated by a ΔA of 0.065. Instead of consuming energy to induce this greater degree of bending, GCLG, GCGG, and GCGR retain fairly high affinity for CRP. Does this contradict the assumption that bending requires energy to stabilize the DNA−protein complex? More bending leads to more extensive contact of the DNA sequence with the protein molecule. Consequently, a sequence defining a stronger propensity to bend leads to better interaction between DNA and CRP. This additional interaction between the flanking sequence and CRP is reflected by an increase in the affinity of DNA−CRP complex formation. This bending propensity is sequence specific. The geometry of the bent complex depends on the context of the total sequence.

Sequence Analysis. From the study of sequence-dependent migration of protein−DNA complexes in nondenaturing polyacrylamide gel electrophoresis, Crothers and co-workers (*14*, *35*) concluded that DNA sequence determines CRP-induced bending and protein binding affinity. A similar result was reported with other DNA binding proteins, e.g., SQUA (*Antirrhinum majus* proteins), a MADS-box family member (*36*). Although the specific CRP binding site is 5 bp for each site with a 6 bp spacer between them, a larger (~30 bp) DNA site is required for full binding strength, implying that extra interactions, either direct or indirect, between the flanking sequence and protein molecule are involved in deforming the trajectory of the double helix. This assumption has been directly confirmed with the X-ray structure of the DNA−CRP cocrystal (*7*). Several lines of evidence from fluorescence study (*15*), X-ray crystallography (*7*), electrophoresis (*1*, *3*), and electric dichroism (*16*) all support the possibility that DNA bends symmetrically in the DNA−CRP complex. However, asymmetrical bending of the *gal* sequence induced by CRP was first reported from fluorescence studies (*21*). On the basis of this observation, the different bending geometry relative to the differences in the molecular mechanism of CRP on class I and class II CRP binding sites has been proposed (*21*). Results of this study confirm that *gal* bends asymmetrically, which is induced by CRP, and the flanking sequence proximal to the TGTGA motif bends more than the other side with an overall bending angle of 95−125°. These data also illustrate that the symmetry of the DNA sequence strongly correlates with CRP-induced bending geometry (Table 5). Does the symmetry in DNA sequence encode the bending geometry and reflect the differences in the molecular mechanism of CRP on class I and class II CRP binding sites? Several natural CRP promoter sites which are categorized as either class I or class II CRP binding sites were analyzed. As shown in Figure 5, two symmetry properties in the *lac* promoter are involved, two half-binding sites being almost symmetric as inverted repeats and the two flanking sequences being almost identical as mirror images. Therefore, in Table 6, both the inverted repeat and mirror image were considered as a symmetry factor in the recognition site and flanking sequence. In class I sequences, ~70% of the nucleotides are either inverted repeats or mirror images of each other through the center dyad axis. In contrast, only 50% of the sequences in class II own this symmetric property. Actually, the value of 50% implies random composition, since DNA consists of only four different bases. Results from the current study indicate that the specific DNA sequence is responsible for the direct and indirect interaction between CRP and DNA on one hand and supplies information for defining the symmetry of DNA bending on the other. In addition, the geometry of the CRP−DNA complex is dependent on promoter type. Thus, these observations support the proposal by Pyles and Lee (*21*) that the geometry of the CRP−DNA complex may play a major role in determining the molecular mechanism in gene expression.

REFERENCES

1. Fried, M. G., and Crothers, D. M. (1983) *Nucleic Acids Res. 11*, 141−158.
2. Kolb, K., Spassky, A., Chapon, C., Blazy, B., and Buc, H. (1983) *Nucleic Acids Res. 11*, 7833−7852.
3. Wu, H.-M., and Crothers, D. M. (1984) *Nature 308*, 509−513.
4. Warwicker, J., Engelman, B. P., and Steitz, T. A. (1987) *Proteins 2*, 283−289.
5. Thompson, J. F., and Landy, L. (1988) *Nucleic Acids Res. 126*, 9687−9705.
6. Zinkel, S. S., and Crothers, D. M. (1990) *Biopolymers 29*, 29−38.

7. Schultz, S. C., Shields, G. C., and Steitz, T. A. (1991) *Science 253*, 1001−1007.
8. Kolb, A., Busby, S., Buc, H., Garges, S., and Adhya, S. (1993) *Annu. Rev. Biochem. 62*, 749−795.
9. Dalma-Weiszhausz, D. D., and Brenowitz, M. (1996) *Biochemistry 35*, 3735−3745.
10. Zhou, Y., Busby, S., and Ebright, R. (1993) *Cell 73*, 375−379.
11. Busby, S., and Ebright, R. H. (1997) *Mol. Microbiol. 23*, 853−859.
12. Zhou, Y., Merkel, T. J., and Ebright, R. H. (1994) *J. Mol. Biol. 243*, 603−610.
13. Zhou, Y., Pendergrast, P. S., Bell, A., Williams, J., Busby, S., and Ebright, R. H. (1994) *EMBO J. 13*, 4549−4557.
14. Gartenberg, M. R., and Crothers, D. M. (1988) *Nature 333*, 824−829.
15. Heyduk, T., and Lee, J. C. (1992) *Biochemistry 31*, 5165−5171.
16. Meyer-Almes, F. J., and Porschke, D. (1997) *J. Mol. Biol. 269*, 842−850.
17. de Crombrugghe, B., Busby, S., and Buc, H. (1984) *Science 224*, 831−838.
18. Fried, M. G., and Crothers, D. M. (1984) *J. Mol. Biol. 172*, 263−282.
19. Heyduk, T., and Lee, J. C. (1989) *Biochemistry 28*, 6914−6924.
20. Heyduk, T., and Lee, J. C. (1990) *Proc. Natl. Acad. Sci. U.S.A. 87*, 1744−1748.
21. Pyles, E. A., and Lee, J. C. (1998) *Biochemistry 37*, 5201−5210.
22. Takahashi, M., Blazy, B., and Baudras, A. (1980) *Biochemistry 19*, 5124−5130.
23. Windholz, M., Ed. (1976) *Merck Index*, 9th ed., Merck & Co., Rahway, NJ.
24. Pyles, E. A., Chin, A. J., and Lee, J. C. (1998) *Biochemistry 37*, 5194−5200.
25. Pyles, E. A., and Lee, J. C. (1996) *Biochemistry 35*, 1162−1172.
26. Lin, S.-H., and Lee, J. C. (2003) *Biochemistry 41*, 14935−14943.
27. Lakowicz, J. (1983) in *Principles of Fluorescence Spectroscopy*, Plunum Press, New York.
28. Cheung, H. C. (1991) in *Topics in Fluorescence Spectroscopy* (Lakowicz, J., Ed.) pp 128−176, Plenum Press, New York.
29. Perrin, F. (1926) *J. Phys. Radium 1*, 390−401.
30. Dean, J. A., Ed. (1979) *Lange's Handbook of Chemistry*, 20th ed., pp 10−97, McGraw-Hill, New York.
31. Lippert, E., Nagelle, W., Seibold-Blakenstein, I., Staiger, U., and Voss, W. (1959) *Analytische Chemie 17*, 1.
32. Grossman, S. H. (1983) *Biochemistry 22*, 5369−5375.
33. Weber, I. T., and Steitz, T. A. (1987) *J. Mol. Biol. 198*, 311−326.
34. Wasylewski, M., Malecki, J., and Wesylewski, Z. (1995) *J. Protein Chem. 14*, 299−308.
35. Dalma-Weiszhausz, D. D., Gartenberg, M. R., and Crothers, D. M. (1991) *Nucleic Acids Res. 19*, 611−616.
36. West, A. G., and Sharrocks, A. D. (1999) *J. Mol. Biol. 286*, 1311−1323.
37. Ebright, R. H. (1993) *Mol. Microbiol. 8*, 797−802.
38. Berg, O. G., and von Hippel, P. H. (1988) *J. Mol. Biol. 200*, 709−723.

BI027259+